DTIC FILE COPY

(2)

TATION PAGE

Form Approved
OMB No. 0704-0188

to average 1 hour per response, including the time for reviewing instructions, searching existing data sources, ewing the collection of information. Send comments regarding this burden estimate or any other aspect of this len. to Washington Headquarters Services, Directorate for Information Operations and Reports, 1215 Jefferson ce of Management and Budget, Paperwork Reduction Project (0704-0188), Washington, DC 20503.

AD-A228 872

DATE	3. REPORT TYPE AND DATES COVERED
	Final Report/01 Mar 87-28 Feb 90

4. TITLE AND SUBTITLE
Applications of Non-Linear Optics

5. FUNDING NUMBERS
61102F/2301/A1

6. AUTHOR(S)
Dana Z. Anderson

7. PERFORMING ORGANIZATION NAME(S) AND ADDRESS(ES)
University of Colorado
Dept of Physics and Joint Institute
for Laboratory Astrophysics
Boulder, CO 80309-0440

8. PERFORMING ORGANIZATION REPORT NUMBER
AFOSR-TR- 90 1103

9. SPONSORING/MONITORING AGENCY NAME(S) AND ADDRESS(ES)
AFOSR/NP
Bolling AFB DC 20332-6448

10. SPONSORING/MONITORING AGENCY REPORT NUMBER
AFOSR-87-0163

DTIC ELECTE NOV 16 1990 S D B

11. SUPPLEMENTARY NOTES

12a. DISTRIBUTION/AVAILABILITY STATEMENT
Approved for public release; distribution is unlimited.

12b. DISTRIBUTION CODE

13. ABSTRACT *(Maximum 200 words)*

Spatial mode-multiplexing is used to transmit several communication channels on a single multimode optical fiber. Each channel is encoded by an orthogonal pattern produced by a spatial light modulator. A photorefractive medium holographically decodes the output speckle pattern at a receiver station. A ring and star architectures for interconnection networks is demonstrated. Typical crosstalk to signal ratios, for fully interconnected 3 processor networks, are -24 and -26 dB for the ring and star respectively.

Keywords: Fiber optics; Optical communications. (RH)

14. SUBJECT TERMS	15. NUMBER OF PAGES
multimode optical fiber, spatial light modulator	18
	16. PRICE CODE: UL

17. SECURITY CLASSIFICATION OF REPORT	18. SECURITY CLASSIFICATION OF THIS PAGE	19. SECURITY CLASSIFICATION OF ABSTRACT	20. LIMITATION OF ABSTRACT
UNCLASSIFIED	UNCLASSIFIED	UNCLASSIFIED	SAR

GENERAL INSTRUCTIONS FOR COMPLETING SF 298

The Report Documentation Page (RDP) is used in announcing and cataloging reports. It is important that this information be consistent with the rest of the report, particularly the cover and title page. Instructions for filling in each block of the form follow. It is important to ***stay within the lines*** to meet ***optical scanning requirements***.

Block 1. Agency Use Only *(Leave blank)*.

Block 2. Report Date. Full publication date including day, month, and year, if available (e.g. 1 Jan 88). Must cite at least the year.

Block 3. Type of Report and Dates Covered. State whether report is interim, final, etc. If applicable, enter inclusive report dates (e.g. 10 Jun 87 - 30 Jun 88).

Block 4. Title and Subtitle. A title is taken from the part of the report that provides the most meaningful and complete information. When a report is prepared in more than one volume, repeat the primary title, add volume number, and include subtitle for the specific volume. On classified documents enter the title classification in parentheses.

Block 5. Funding Numbers. To include contract and grant numbers; may include program element number(s), project number(s), task number(s), and work unit number(s). Use the following labels:

C	- Contract	**PR**	- Project
G	- Grant	**TA**	- Task
PE	- Program Element	**WU**	- Work Unit Accession No.

Block 6. Author(s). Name(s) of person(s) responsible for writing the report, performing the research, or credited with the content of the report. If editor or compiler, this should follow the name(s).

Block 7. Performing Organization Name(s) and Address(es). Self-explanatory.

Block 8. Performing Organization Report Number. Enter the unique alphanumeric report number(s) assigned by the organization performing the report.

Block 9. Sponsoring/Monitoring Agency Name(s) and Address(es). Self-explanatory.

Block 10. Sponsoring/Monitoring Agency Report Number. *(If known)*

Block 11. Supplementary Notes. Enter information not included elsewhere such as: Prepared in cooperation with...; Trans. of...; To be published in.... When a report is revised, include a statement whether the new report supersedes or supplements the older report.

Block 12a. Distribution/Availability Statement. Denotes public availability or limitations. Cite any availability to the public. Enter additional limitations or special markings in all capitals (e.g. NOFORN, REL, ITAR).

- **DOD** - See DoDD 5230.24, "Distribution Statements on Technical Documents."
- **DOE** - See authorities.
- **NASA** - See Handbook NHB 2200.2.
- **NTIS** - Leave blank.

Block 12b. Distribution Code.

- **DOD** - Leave blank.
- **DOE** - Enter DOE distribution categories from the Standard Distribution for Unclassified Scientific and Technical Reports.
- **NASA** - Leave blank.
- **NTIS** - Leave blank.

Block 13. Abstract. Include a brief *(Maximum 200 words)* factual summary of the most significant information contained in the report.

Block 14. Subject Terms. Keywords or phrases identifying major subjects in the report.

Block 15. Number of Pages. Enter the total number of pages.

Block 16. Price Code. Enter appropriate price code *(NTIS only)*.

Blocks 17. - 19. Security Classifications. Self-explanatory. Enter U.S. Security Classification in accordance with U.S. Security Regulations (i.e., UNCLASSIFIED). If form contains classified information, stamp classification on the top and bottom of the page.

Block 20. Limitation of Abstract. This block must be completed to assign a limitation to the abstract. Enter either UL (unlimited) or SAR (same as report). An entry in this block is necessary if the abstract is to be limited. If blank, the abstract is assumed to be unlimited.

A Report to the
Air Force Office of Scientific Research

1 March 1987 - 28 February 1990
Grant #AFOSR-87-0163

Submitted by

Dana Z. Anderson
Department of Physics and
Joint Institute for Laboratory Astrophysics
University of Colorado, Boulder, CO. 80309-0440

Multimode Fiber Communications Channel Multiplexing Scheme

We have completed work on the fiber optic bus. We briefly describe its principles here: a complete description may be found in the attached preprint which will be submitted for publication.

A multimode fiber illuminated with light from a monochromatic source produces a complicated speckle pattern that arises from the interference of many fiber modes. It is difficult if not impossible to say specifically what the output pattern will be, especially if the number of propagating modes is very large. Suppose the fiber is illuminated with two different optical fields that are electric-field orthogonal at some input reference plane. Even not knowing their spatial distribution, the two output patterns are guaranteed to be field amplitude orthogonal, provided there is no light lost between the input plane and the output. The orthogonality is guaranteed by the unitarity of the fiber, viewed mathematically as an energy preserving linear transformation operator. Even if there is modest loss, in many cases the outputs will be orthogonal, or nearly so.

Two speckle patterns produced by sources at *different* locations along a single fiber are not guaranteed to be orthogonal. The expectation value of the overlap of two randomly chosen equal intensity speckle patterns of an N mode fiber is 1/N. For N large, the probability that the overlap deviates from its expected value drops off so sharply with the deviation that for some practical purposes the patterns may be taken to be orthogonal. For example, for a fiber carrying 10,000 modes and 100 random patterns, the probability that *any two* patterns have an overlap integral greater than 0.1 is $P<10^{-220}$!

We have now demonstrates a technique for signal multiplexing on a multimode fiber which is based on the unitarity principle and which capitalizes on the high dimensionality of speckle patterns. Time signals are encoded by their spatial amplitude and phase pattern at the transmitter. They are decoded by a dynamic volume hologram, formed by interfering the output speckle pattern with itself at the receiver. Speckle patterns derived from input patterns orthogonal to the ones used to write the hologram will not give rise to a strong reconstructed object beam. That the hologram is dynamic ameliorates the obvious problem of fiber movement, for if it moves a substantial amount, the speckle pattern for a given input changes, but the hologram can be refreshed. It also allows the interconnects between a collection of transmitters and receivers to be reconfigurable.

The system we constructed works very well, and a patent disclosure in currently being developed. Several experiments were executed to test the properties of this system. For example, we demonstrated the unitarity principle by translating an illuminated slit, with the light from the slit injected into the multimode fiber. A hologram is written with the slit in one position,

then the slit is translated and the diffracted light observed. As a function of the position of the slit from it initial one, we saw the diffracted intensity decrease much as expected, as shown in figure [2] of the preprint. We also say the diffracted intensity decrease as $\cos^2(\theta)$ as the polarization of the input light was rotated. Both these are excellent confirmations of the principles of the technique.

We have also constructed both a ring and a star optical bus structure with three transmitter and receiver stations. Again, results are described more fully in the attached article.

Hill gratings for SHG enhancement in fibers

Reflective (Hill) gratings and SHG in optical fibers have been connected by their common dependence on the dopant germanium. This connection as well as the common theory we were using to describe the two effects prompted us to try an experiment in which reflective gratings would provide the source of SHG. This would produce SHG capability almost instantly, as opposed to the usual preparation method, which requires high-power IR light to be launched into the fiber for hours. After many runs covering a wide range of parameters, very little enhancement of SHG was found. The maximum effect was a factor of four increase over the weak SH initially present in the fiber. This is very small when compared to the normal method of preparing SHG in fibers, where the SH grows to over a million times its initial value. At this point, the small enhancement is attributed the the difficulty of the experiment.

We proceeded with experiments on fibers with high germanium concentrations. We found higher levels of initial SH, but the saturated levels of SH were equivalent to those found using fibers containing little germanium. The final conversion efficiency is most strongly dependent upon the phosphorus content and annealing history of the fibers, which help determine the number of fiber defect centers available for phasematched SHG. The high initial SH seen in the high Ge-doped fibers is probably due to the larger than normal index change at the core-cladding interface. The initial SH is believed to come from quadrupole interactions at this interface.

The behavior of SHG in fibers at different temperatures is also being investigated. Prepared SHG fibers have been heated to as much as 1000°C to see if this causes any change in the SH. When cooled back to room temperature, we see little change in the SHG strength. This means that whatever is providing the $\chi^{(2)}$ source term is stable up to thermal energies of around 1/10 eV. At these energies, most of the defect centers in the fiber should anneal out. Our experiments show that, while defect centers may be associated with SHG, they are not the sole source of the nonlinearity. We are currently making a stable mount for the fiber oven to facilitate preparation of fibers at elevated temperatures. The growth rate of SH in the fiber could indicate where the $\chi^{(2)}$ source term comes from and ways that it could be enhanced.

Photorefractive Hill Gratings

The Hill Grating formation mechanism is not fully understood, although several models and theories have been worked out. One model we have pursued is based on the defects induced by laser light in Ge-doped glass which was used for second harmonic generation in the optical fibers before. Now, we considered the same kinds of defects, Ge(1), Ge(2) and Ge E' centers, optically induced and aligned during the process of preparing this photosensitive grating in the fibers. Then we treated this permanent dipole system as a 2-level system, calculated the density matrix from the first order to forth order using perturbation theory, then the complex polarization and index change. Finally, using self consistency equations found the time dependent reflectivity. The early result, refractive index change was about the order of 10^{-6}, reflectivity R(t) is

proportional to $(1+e^{-at})^{-2}$, agreed with the experimental curves. This work will help us to understand the origin of the Hill Grating formation.

In the last annual report, we reported our preliminary observation of the intensity threshold of the Hill Grating formation in Ge-doped optical fibers. We are in the process of measuring this threshold more accurately. The fibers we used is D type polarization preserving fiber with core size 1 by 2 microns from Andrew Corp., cleaved to different lengths, 1.5, 4, 14, 28 and 50 cm, one dozen of each length. Then we write one grating with each intensity in each fresh fiber using single mode argon laser beam at 488 nm or 515 nm isolated from fiber end reflection by an acoustooptic modulator. The fiber is coiled in a copper fiber holder which is temperature controlled to a few millidegrees Kelvin, cooled somewhat below room temperature. We have constructed an alignment system which stabilizes the pointing of the laser beam. In this experiment, to exclude the etalon effect from both fiber ends, we tried to tilt one fiber end about seven-degree angle, but the end quality was not as good as cleaved one, then we designed a seven-degree 'gel prism' which was filled with index matching gel, but the long time stability was not as good as we expected; we attribute the stability problems to creep of the gel.

Grating formation commences at an intensity in the range from one to 30 mW depending on the length of the fiber and on the initial intensity of the light reflected from the output end. The threshold behavior resembles that observed for self-seeded growth of second-harmonic light: below the threshold no grating is written, above threshold, grating formation begins, but reducing the light intensity below threshold stops further growth. The threshold may be due to a balance between gain and loss for the growth process; it could also be indicative of the underlying physics/chemistry of the excitation mechanism.

We also tried to write the enhanced grating using a back end mirror. At beginning, we used silvered back fiber end, the problem was that at high intensity level the silver was burnt. Then we used a back end mirror (need fiber back end movable, otherwise the fiber end would be knocked off by the mirror). The reflectivity can be much higher than that of without back mirror, a 1.5 cm piece of E fiber from Andrew Corp., for example, from 19% going up to 76%.

In future work we will continue to work on the above theory and experiments, and try to observe the refractive index change in the fibers.

Mode-multiplexing and holographic demultiplexing communication channels on a multimode fiber

Mark Saffman and Dana Z. Anderson

Department of Physics and Joint Institute for Laboratory Astrophysics
University of Colorado, Boulder, CO. 80309-0440

Spatial mode-multiplexing is used to transmit several communication channels on a single multimode optical fiber. Each channel is encoded by an orthogonal pattern produced by a spatial light modulator. A photorefractive medium holographically decodes the output speckle pattern at a receiver station. We demonstrate ring and star architectures for interconnection networks. Typical crosstalk to signal ratios, for fully interconnected 3 processor networks, are -24 and -26 dB for the ring and star respectively.

Thursday, October 4, 1990

A multimode fiber illuminated with light from a monochromatic source produces a complicated speckle pattern that arises from the interference of many fiber modes[1]. It is difficult if not impossible to say specifically what the output pattern will be, especially if the number of propagating modes is very large. Suppose the fiber is illuminated with two different optical fields that are electric-field orthogonal at some input reference plane. Even not knowing their spatial distribution, the two output patterns are guaranteed to be field amplitude orthogonal, provided there is no light lost between the input plane and the output. The orthogonality is guaranteed by the unitarity of the fiber, viewed mathematically as an energy preserving linear transformation operator[2]. Even if there is modest loss, in many cases the outputs will be orthogonal, or nearly so.

Two speckle patterns produced by sources at different locations along a single fiber are not guaranteed to be orthogonal. The expectation value of the overlap of two randomly chosen equal intensity speckle patterns of an N mode fiber is 1/N. For N large, the probability that the overlap deviates from its expected value drops off so sharply with the deviation that for some practical purposes the patterns may be taken to be orthogonal. For example, for a fiber carrying 10,000 modes and 100 random patterns, the probability that *any two* patterns have an overlap integral greater than 0.1 is $P<10^{-220}$!

In this paper we demonstrate a technique for signal multiplexing on a multimode fiber[3,4] which is based on the unitarity principle and which capitalizes on the high dimensionality of speckle patterns. Time signals are encoded by their spatial amplitude and phase pattern at the transmitter. They are decoded by a dynamic volume hologram[5], formed by interfering the output speckle pattern with itself at the receiver[6]. Speckle patterns derived from input patterns orthogonal to the ones used to write the hologram will not give rise to a strong reconstructed object beam. That the hologram is dynamic ameliorates the obvious problem of fiber movement, for if it moves a substantial amount, the speckle pattern for a given input changes, but the hologram can be

refreshed. It also allows the interconnects between a collection of transmitters and receivers to be reconfigurable[7].

The principle of the technique is easily demonstrated by injecting the light transmitted by a mask with a rectangular hole into a multimode fiber, as shown in Fig. 1. A volume hologram is made with this light, then, as the mask is translated the holographically diffracted light intensity will decrease, as illustrated in Fig. 2. Ideally when the mask has been translated a distance greater than its width the diffracted intensity should drop to zero. Similar results were obtained using a 70 meter length of fiber wrapped on a 15cm diameter spool and having ~50% transmission loss, although the background signal, with the mask completely displaced, was about twice as high. We have also observed the same behavior when varying the electric field polarization angle: rotating the polarization by θ from that used to write the hologram causes the diffracted light to decrease as $\cos^2(\theta)$.

Fig. 3. shows that the discrimination against orthogonal spatial patterns improves as the grating strength increases, up to the point where beam fanning degrades the results. However, a signal to crosstalk ratio of better than 50:1, or 34 dB after detection, can be realized for 45% diffraction efficiency gratings.

We have constructed ring and star interconnection networks, each having three transmitter/receiver nodes, as shown in Fig. 4. Each transmitter has an acoustooptic modulator to produce an intensity modulated signal and a spatial light modulator to encode the signal on a given channel. In our case, the light "modulator" is simply a piece of glass, mounted at an oblique angle to the beam, which, when rotated, selects an input angle to the fiber. The beam numerical aperture was ~0.02, compared to 0.3 for the step index fiber. The receiver at each node of the ring network uses a polarizing beamsplitter to separate the polarization components of the speckle pattern, thereby producing two speckle patterns. The interference pattern produced over the entire

intersection of the two speckle patterns is recorded in a photorefractive crystal. The star network uses a single photorefractive crystal to perform the interconnects as shown in Fig. 4b. Normally the signals would be coupled back into multimode fibers for propagation to the receivers; in the experiment we simply have detectors at the output from the hologram.

The ring and star architectures are in many ways complementary. For a fully interconnected N node network the ring requires storing O(N) holograms in N separate crystals, whereas the star stores $O(N^2)$ holograms in a single crystal. The star places higher demands on the holographic medium, but eliminates the loss at the passive node couplers[8], inherent to the ring architecture. In the ring architecture the transmitters may be mutually incoherent, but in the star the interconnects are formed by the interference of patterns from separate nodes, so all transmitters must be mutually coherent. In both structures, the switching speed is limited by the spatial light modulator response time, once the interconnection holograms have been recorded.

The ring network interconnections were written for each node sequentially. For example two 5% efficiency holograms were recorded at node 1 by sequentially transmitting pattern 1 from nodes 2 and 3. Worst case crosstalk, defined as the diffracted signal at a node relative to the undesired signal due to the same node simultaneously transmitting, was measured at each node. Typical crosstalk levels were -25 and -22 dB, after detection, for transmission to nearest and next-nearest neighbor nodes respectively.

The star network was initialized by having pairs of nodes transmit simultaneously. The signals from the intended transmitter and receiver nodes were then selected as reference and object beams respectively. To fully interconnect the three node network the exposure times were varied from 10.6 to 6 seconds[9] to write six equal strength holograms of ~5% diffraction efficiency. The typical switching performance with two simultaneous talkers is shown in Fig. 6. Crosstalk levels

were measured for each set of interconnections. The spread, due to small variations in the strength of the holograms, was from -24 to -27 dB, with an average of -26 dB.

In a communication system based on this technique we have two choices for the laser source: the entire network can be supplied by a single high power source (as we have done) or each transmitter can have its own source. In the case of a single source we are free to supply a "nice" object beam, which would be ideal from a holography standpoint. Recording the interference between two speckle patterns is in many respects an odd thing to do, but it does permit, for example, the source lasers to be mutually incoherent.

Under the proper circumstances the volume hologram can provide a measure of the amplitude overlap, that is, the dot-product between a write and a read beam along one spatial dimension[10]; ideally, one would use a waveguide that is single mode in one dimension and multimode in the other. In our configuration then, the effective number of modes is the square-root of the number of modes (per polarization direction) of the two-dimensional fiber. Even in the one-dimensional case, we know little about the properties of superimposed holograms written with pairs of speckle patterns. We do know, for example, that a single such hologram is not linear in the product of the fields because both beams are amplitude modulated and therefore the recording medium time constant will be space dependent. In any case, we expect that it is the holographic aspects that will limit the channel carrying capacity of the scheme, not the fiber itself.

In any practical version of these networks the dynamic recording medium needs to be periodically updated. The holograms erase while being used and any mechanical perturbations to the fibers cause fluctuations in the mode patterns, leading to reduced diffraction efficiency and increased crosstalk. We note that the ring architecture is relatively insensitive to fiber movement since each hologram is derived from a single speckle pattern. To avoid dead time, we envision a twin bus structure that uses one bus while the holographic media of the other are refreshed. It may

be helpful in a practical device to employ a high speed photorefractive material such as BSO or GaAs.

The authors are grateful to C. Benkert for fruitful discussions. This work was supported by the Air Force Office of Scientific Research, Grant #AFOSR-90-0198. M.S. would like to acknowledge support provided by a fellowship from the NSF Engineering Research Center in Optoelectronic Computing Systems at the University of Colorado and an AFOSR laboratory graduate fellowship. D. Z. A. is an Alfred P. Sloan Research Fellow.

References

1. For an interesting discussion on fiber modes, see A. Yariv, J. Opt. Soc. Amer., **66**, 301 (1976).

2. On unitarity see, for example, L.D. Landau and E.M. Lifshitz, *Quantum Mechanics, Non-Relativistic Theory*, 2nd ed., p.35, Pergamon Press, Oxford, (1965).

3. For a description of other fiber multiplexing techniques see, A.B. Sharma, S.J. Halme and M.M. Butusov, *Optical Fiber Systems and Their Components*, Springer-Verlag, Berlin, (1981).

4. Related work on spatial mode-multiplexing, which was however limited to fibers without mode coupling, has been reported by S. Berdague and P. Facq, Appl. Opt., **21**, 1950 (1982).

5. L. Solymar and D.J. Cooke, *Volume Holography and Volume Gratings*, Academic Press, London, (1981).

6. Holographic detection for fiber sensors has been used by: T.J. Hall, M.A. Fiddy and M.S. Ner, Opt. Lett., **5**, 485, (1980); and by G. Indebetouw, K.D. Bennett, P. Zhang and R.G. May, J. Lightwave Tech., **8**, 1039 (1990).

7. For a recent review of the field see J.W. Goodman, "Optics as an interconnect technology", in *Optical Processing and Computing* eds. H.H. Arsenault, T. Szoplik and B. Macukow, Academic Press, Boston, (1989).

8. The fused coupler losses are approximately mode independent, so field orthogonality, but not unitarity, is preserved.

9. K. Bløtekjær, Appl. Opt., **18**, 57 (1979).

10. D.Z. Anderson and D.M. Lininger, Appl. Opt., **26**, 5031 (1987).

Figure Captions

Fig. 1. Mode-multiplexing in multimode fiber. The fiber is step index, 100μ core, 50 cm long. Receiver: PBS=polarizing beam splitter, S=shutter, f_1=20 mm, f_2=40 mm, the $LiNbO_3$ is 6mm thick and doped with 0.015% weight Fe and the beam overlap region is ~0.2 x 0.2 x 1.1 mm^3.

Fig. 2. Variation of diffracted signal with input pattern. The calculated lines correspond to the area overlap of two displaced rectangles, and therefore do not account for diffraction from the edges.

Fig. 3. Diffraction efficiency and crosstalk vs. exposure time for a single hologram. Crosstalk is defined as diffracted signal from orthogonal input pattern/diffracted signal from original input pattern. Writing intensity =0.7 W/cm^2.

Fig. 4. Ring and star optical interconnection networks. a) the ring nodes are connected to the network with symmetric multimode couplers , b) the star uses a single interconnection crystal as an optical crossbar. The fiber coupler is a x10 microscope objective, B.Sel.=beam selector, f=40 mm and the beam overlap region is ~0.9 x 0.9 x 5.1 mm^3.

Fig. 5. Data switching in the star network with two simultaneous talkers. Nodes 1 and 2 transmit at 23 and 160 kHz. In a) 1 talks to 2 and 2 talks to 1. In b) 1 talks to 1 and 2 talks to 2.

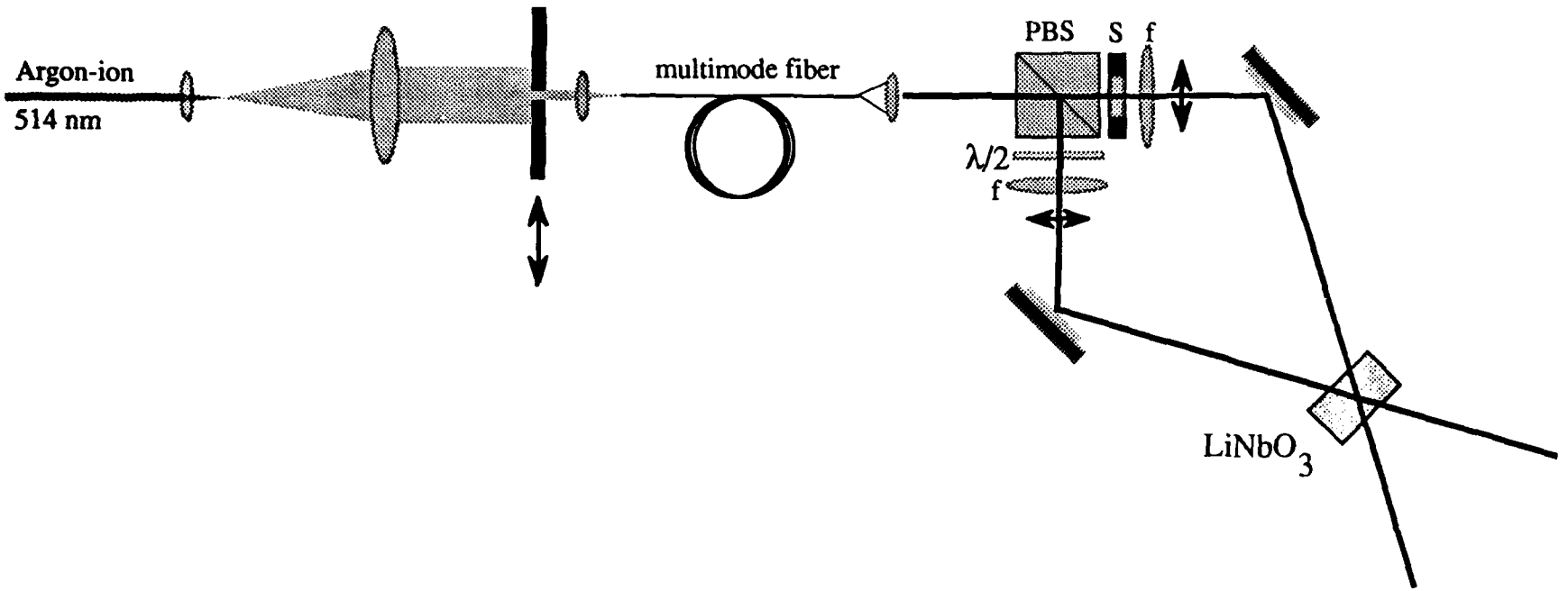

Saffman and Anderson
Mode-multiplexing and holographic...
Figure 1

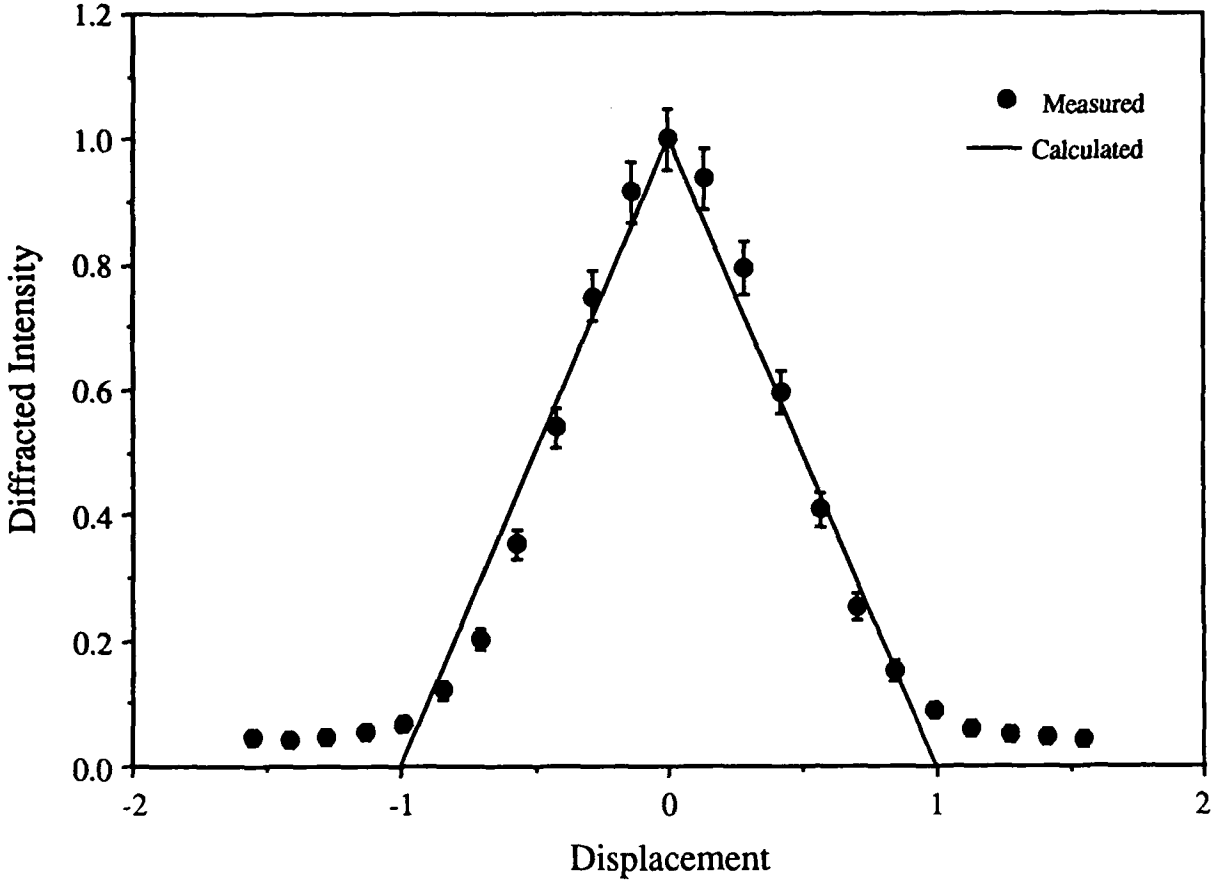

Saffman and Anderson
Mode-multiplexing and ...
Figure 2

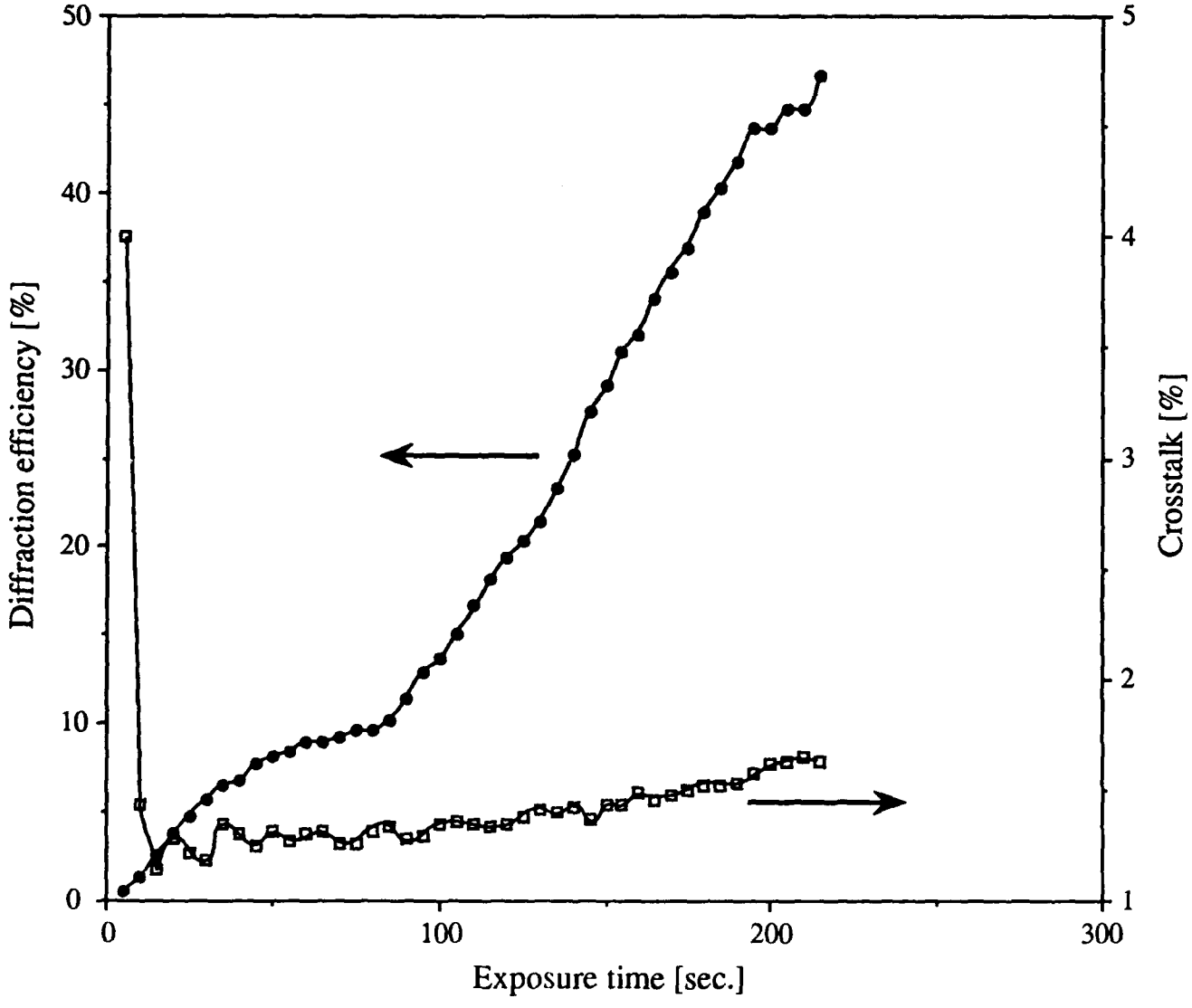

Saffman and Anderson
Mode-multiplexing and ...
Fig. 3

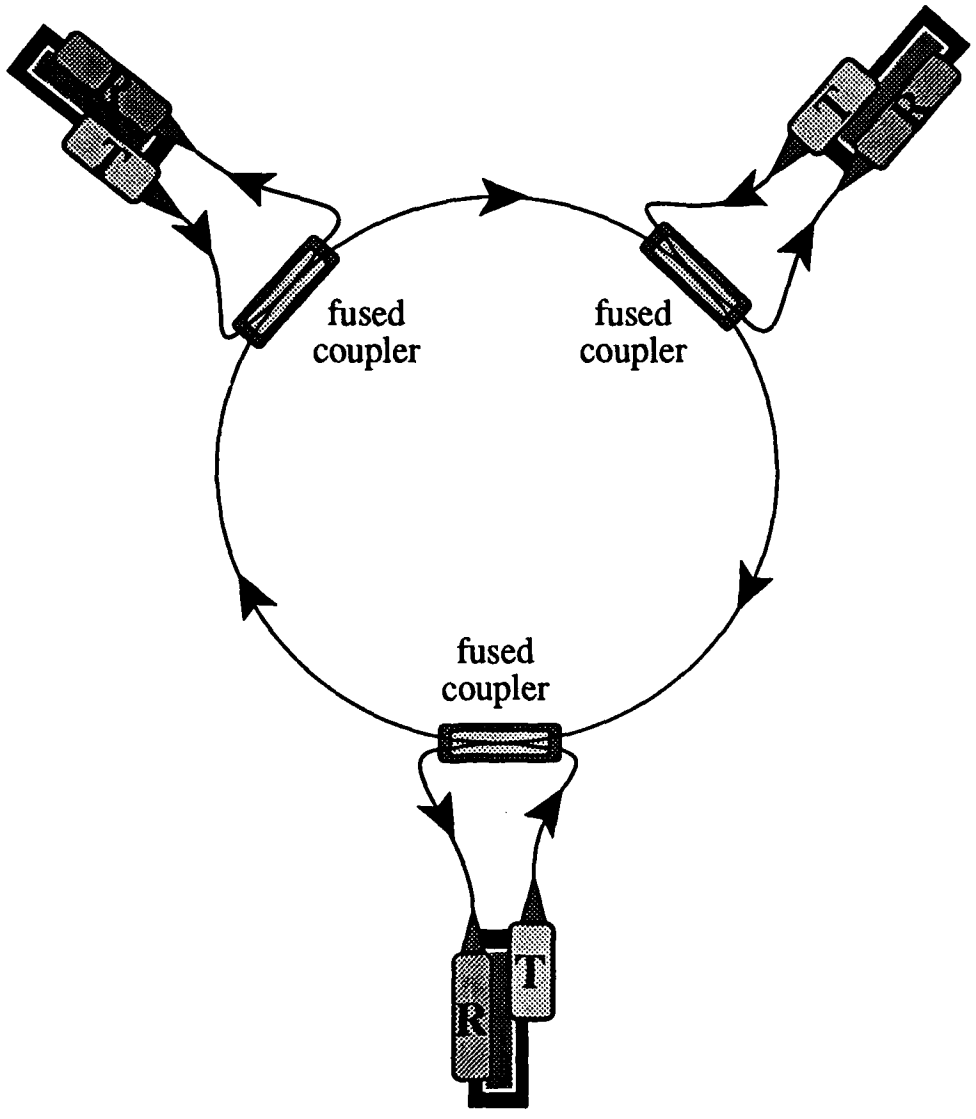

Saffman and Anderson
Mode-multiplexing and holographic...
Figure 4a

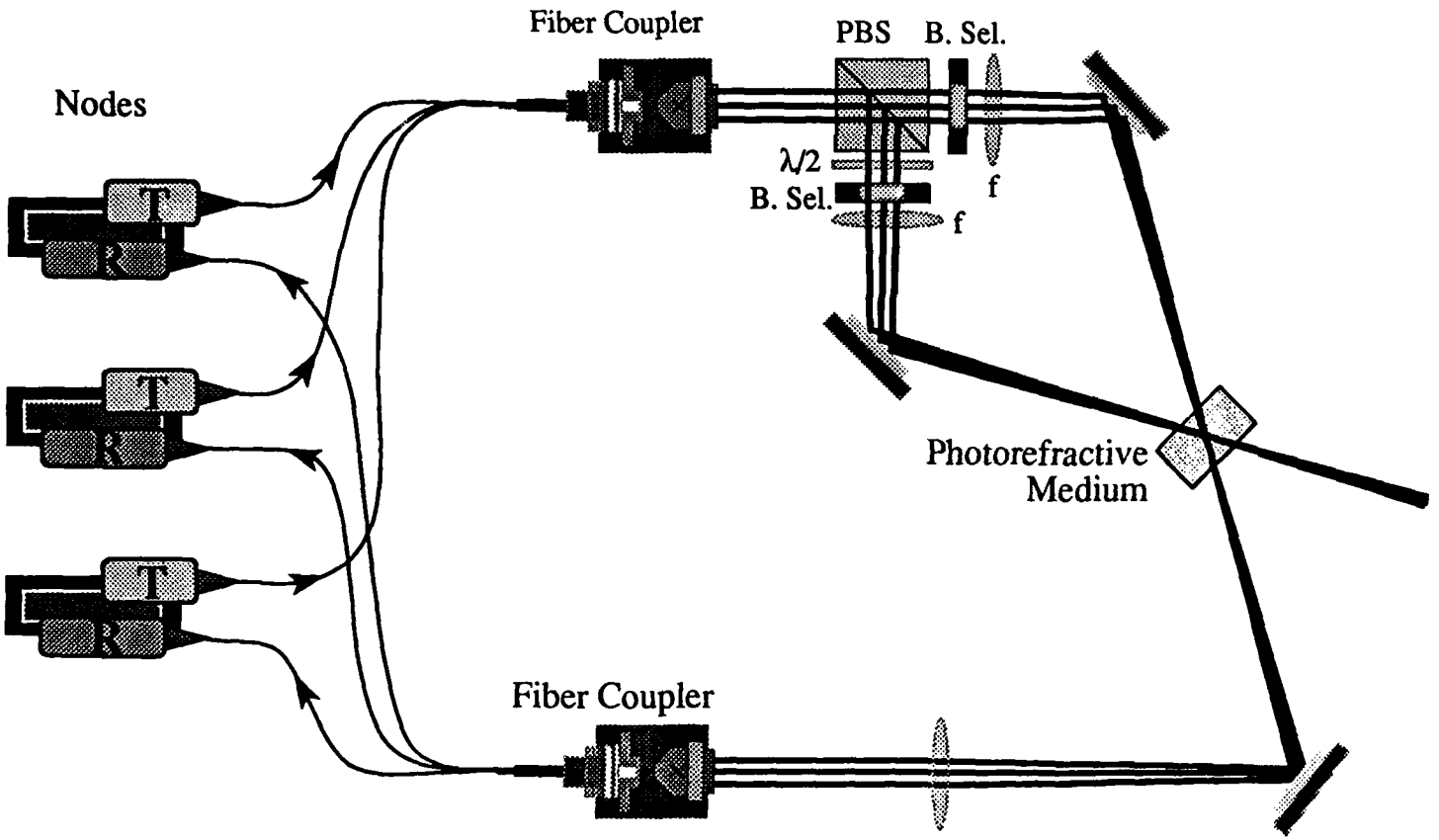

Saffman and Anderson
Mode-multiplexing and holographic
Figure 4b

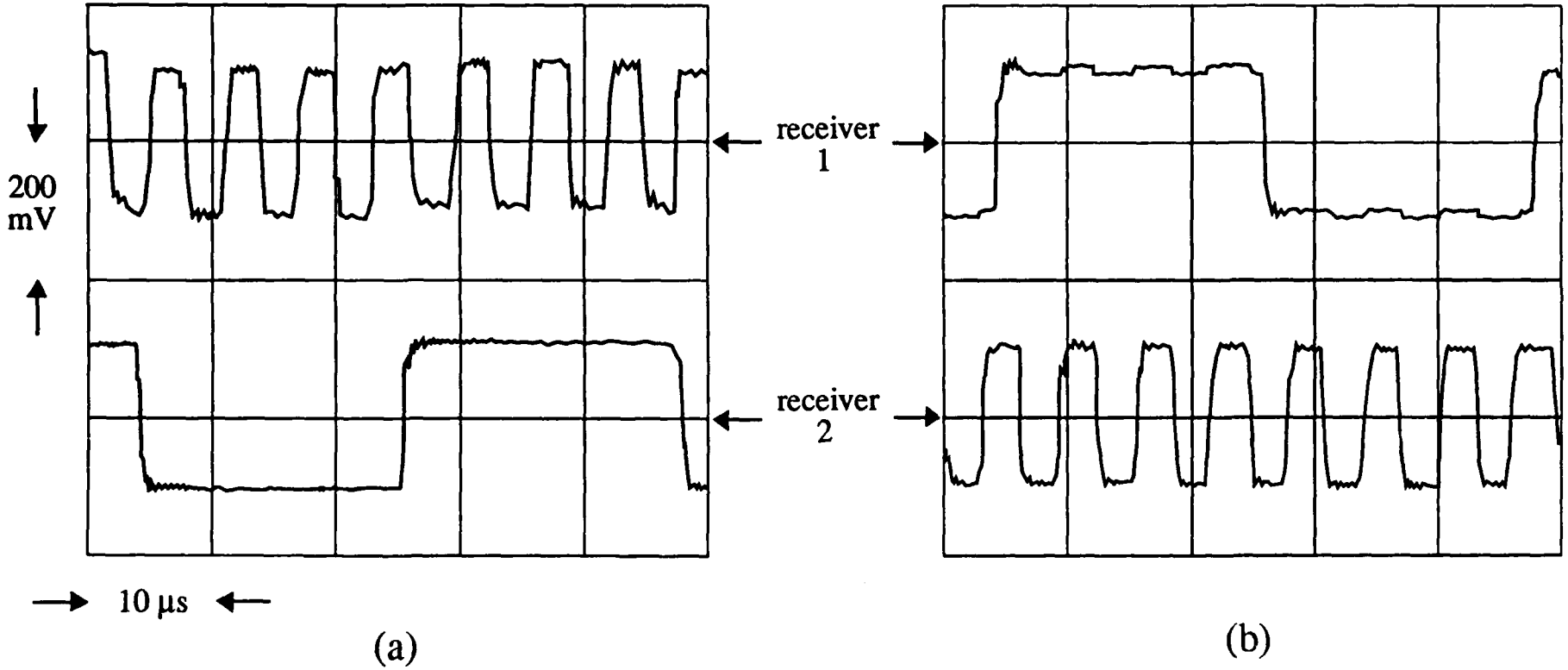

Saffman and Anderson
Mode-multiplexing and holographic...
Figure 5